Eur Spine J (2011) 20:1225–1232
DOI 10.1007/s00586-011-1704-y

ORIGINAL ARTICLE

A fresh look at the nucleus-endplate region: new evidence for significant structural integration

Kelly R. Wade · Peter A. Robertson · Neil D. Broom

Received: 18 May 2010 / Revised: 17 January 2011 / Accepted: 20 January 2011 / Published online: 15 February 2011

Abstract The disc nucleus is commonly thought of as a largely unstructured gel. However, exactly how the nucleus integrates structurally with the endplates remains somewhat ambiguous. The purpose of this study was to investigate whether a substantial level of structural/mechanical cohesion does, in fact, exist across the nucleus-endplate junction. Vertebra–nucleus–vertebra samples were obtained from mature ovine lumbar motion segments and subjected to a novel technique involving circumferential transverse severing (i.e. ring-severing) of the annulus fibrosus designed to eliminate its strain-limiting influence. These samples were loaded in tension and then chemically fixed in order to preserve the stretched nucleus material. Structural continuity across the nucleus-endplate junctions was sufficient for the samples to support, on average, 20 N before tensile failure occurred. Microscopic examination revealed nucleus fibres inserting into the endplates and the significant level of load carried by the nucleus material indicates that there is some form of structural continuity from vertebra to vertebra in the central nucleus region.

Keywords Disc nucleus · Cartilaginous endplate · Fibrosity · Tethering mechanisms

K. R. Wade · N. D. Broom (✉)
Tissue Mechanics Laboratory,
Department of Chemical and Materials Engineering,
University of Auckland, Auckland, New Zealand
e-mail: nd.broom@auckland.ac.nz

P. A. Robertson
Department of Orthopaedic Surgery,
Auckland Hospital, Auckland, New Zealand

Introduction

The disc, consisting of three main components—the nucleus, the annulus, and the cartilaginous endplates—provides a strong but flexible linkage between adjacent vertebrae. The nucleus is surrounded by the concentric annular layers or lamellae with each comprising parallel arrays of collagen fibres crossing obliquely at alternating angles between adjacent layers. The annulus and nucleus are contained superiorly and inferiorly between the cartilaginous endplates, the latter, in turn, structurally linked to the vertebral bodies via the vertebral endplates. Under compression, the nucleus, enclosed by the annulus, is loaded hydrostatically, and by expanding against the walls of the annulus, transfers compressive loads into the annulus [1–8].

The annulus has been extensively studied by many researchers. Tensile testing has been used to determine the bulk mechanical properties of the annular wall. However, the highly directional arrangement of fibres within each layer means that considerable care must be taken to ensure that test samples are prepared such that fibre orientation incorporation within the sample does actually reflect the true strength contribution of these fibres [9–12].

Our own research group has used a variety of combined micromechanical and microstructural techniques to investigate the subtler aspects of disc microanatomy and its functional implications. By stretching carefully orientated sections of fully hydrated annulus either across or along the primary in-plane fibre direction and simultaneously viewing microstructural responses, a number of important structural features in the disc have now been identified. Specifically, both fibrillar interactions within and between layers have been demonstrated and an extensive interlamellar bridging network has been identified which has

implications for explaining interlamellar cohesion in the annulus and hence its mechanical properties [13–16].

In contrast, little consideration seems to have been given to the extent to which the nucleus is integrated with the endplates or even the annulus. Although much of the literature seems to suggest that the non-degenerate nucleus is largely an amorphous, gelatinous structure, several researchers have identified a sparse network of elastin fibres within the nucleus [17–19]. Some ultrastructural studies have concluded that there is no significant attachment between the nucleus and the cartilaginous endplate [20–22]. Other authors suggest that while there is some connection between the nucleus fibres and the cartilaginous endplate, it is via a poorly organised structure [23]. Another view is that the nucleus is a much smaller mid-disc-height structure that is not connected to the cartilaginous endplates at all. Rather, the nucleus is totally contained by the inner annulus fibres which sweep around it and insert directly into the central endplate region [24, 25].

With the above structural ambiguities in mind, the primary aim of this new investigation was to explore the nature of any structural relationship between the nucleus and the cartilaginous endplates.

Methods

General

Thirteen ovine lumbar spines, dissected from freshly slain mature animals (ewes), were wrapped in plastic film and stored at −20°C for no longer than 3 months. In preparation for testing, the extraneous soft tissues and posterior elements were removed from each spine. The vertebrae were then bisected centrally to isolate the discs and their adjacent vertebrae. A composite block of tissue consisting primarily of vertebra–nucleus–vertebra was carefully sawn from each motion segment while in its frozen state and then thawed. It should be noted that this initial preparation did, unavoidably, leave some residual annular elements (see plan view in Figs. 1, 2a).

Mechanical assessment

An assessment of the tensile properties of the extracted vertebra–nucleus–vertebra sample was conducted on 12 samples from 4 spines using the following procedure: each sample was mounted between the plinths of an Instron 5543 testing machine fitted with a 1,000-N load cell. Tissue glue was used for this mounting procedure whilst ensuring that the sample was not subjected to any bending moment, i.e. only an axial tensile load was applied. All 12 tests were carried out with a crosshead displacement rate of 0.5 mm/min. Loading was terminated at approximately 30–40 N, due to the limitations of the sample attachment method; this resulted in axial extensions within the disc tissue of no more than ∼1.5 mm. Each sample was kept hydrated with physiological saline throughout the testing procedure.

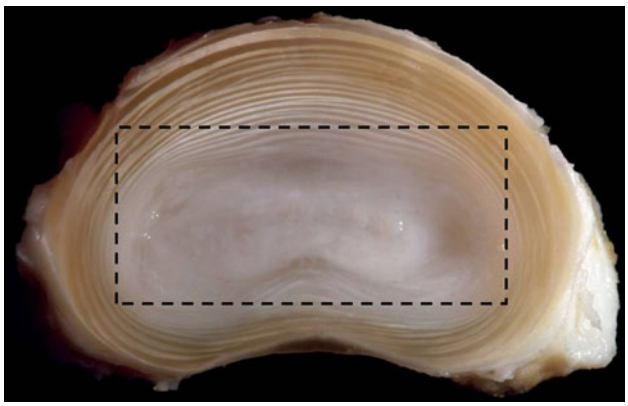

Fig. 1 Transverse cross section of an ovine intervertebral disc, with the annulus and nucleus clearly visible. The *boxed region* shows the approximate outline of the vertebra–nucleus–vertebra sample cut from the motion segment and then subsequently ring-severed. (image courtesy of Dr Sam Veres)

The sample was unloaded and then temporarily detached from the testing machine whilst retaining the ability to relocate it in exactly the same position for further testing. The residual annular elements were then carefully and progressively ring-severed, their complete severance indicated by a sudden, large increase in both extension and mobility of the remaining nucleus material. The ring-severed sample was then remounted in the testing machine and retested at the same displacement rate used previously. All tests on these 12 ring-severed samples were taken to near failure. The results from the tensile testing were presented as raw load–displacement curves (as opposed to stress–strain curves) due to the difficulties of obtaining an accurate measurement of the dimensions of the ring-severed sample, especially during the later stages of the test. Employing this procedure meant that accurate comparisons of response were confined to the unsevered versus severed states within each sample, rather than between samples.

Microstructural assessment

For the microstructural studies, a further 11 vertebra–nucleus–vertebra samples were subjected to ring-severing only, and then manually stretched, followed by chemical fixation in their stretched state, and finally decalcified. From prior experimentation it was found that the remaining nucleus mass could be extended up to five times its original axial height (i.e. up to 500% strain) before reaching a

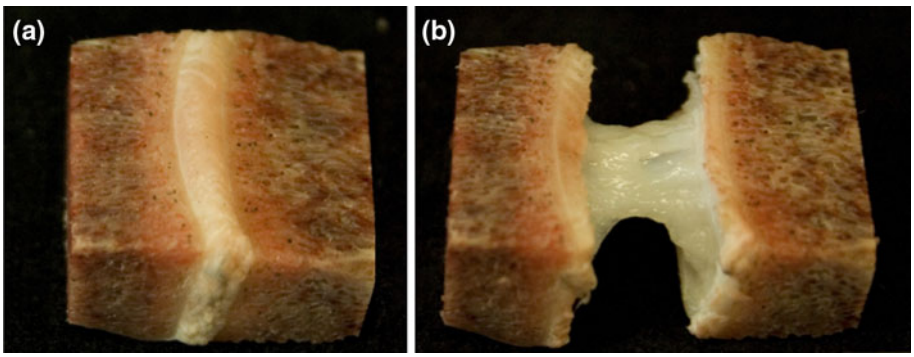

Fig. 2 **a** The extracted vertebra–nucleus–vertebra sample, before ring severing and tensile loading. **b** The same sample after ring severing and tensile stretching. Note the dramatic difference in the length of the unsevered (**a**) versus the severed, then stretched sample (**b**)

limiting extension beyond which progressive failure occurred (see Fig. 2b). Each of the 11 ring-severed samples was held in this highly stretched but unruptured state by applying a minor load of approximately 1 N, sufficient to maintain the nucleus material in its near strain-limiting state (see Fig. 2b) followed by fixation for 3 days in 10% formalin and decalcification for 14 days in 10% formic acid.

All samples for microstructural analysis were then appropriately trimmed and 30-μm thick sagittal sections obtained by cryosectioning. These sections were then wet-mounted on slides and examined using differential interference contrast optical microscopy (DIC). In addition, to obtain clearer differentiation between the nucleus and inner annulus, three intact motion segments were fixed, decalcified, and sectioned sagittally, and then examined using DIC. A total of 26 motion segments from 13 ovine lumbar spines were used in the study.

Results

Figure 3 shows a typical low magnification view of a sagittal section taken from an untrimmed (i.e. intact) vertebra–disc–vertebra sample. The dotted red lines indicate the approximate degree of ring-severing, i.e. the radial extent to which the strain-limiting annular fibres were rendered inoperative. Figure 4 shows a set of typical load/displacement responses obtained from a sample prior to its ring-severing (curve A) and then following its ring-severing and extended to complete failure (curve B). For the 12 samples tested to failure the mean peak load carried by the ring-severed samples was 20 N (range 10–32 N). Edge measurements conducted on all prepared samples indicated a disc height of 3–3.5 mm ($N = 10$) prior to any tensile loading. Note especially the greatly increased level of axial extension of the ring-severed disc before rapid stiffening occurred at around 3–4 mm of extension (see region marked J on curve B).

Figure 5 shows a low-magnification sagittal view of the ring-severed sample stretched to around 350% of its original length and fixed in this state. Two points should be noted with respect to this image: First, it reveals the greatly increased amount of extension that is now possible as a consequence of severing the strain-limiting annular wall elements. Hence, what we are now seeing in this image is a more unravelled form of the central nucleus mass. While this central mass still contains a significant amount of convoluted/folded fibrous content (see region A in Fig. 5 and the enlarged view in Fig. 6), the mass edges are much more axially aligned and appear to exhibit endplate-to-endplate continuity which, in the image shown, is especially clear on the RHS (see boxed region B in Fig. 5 and enlarged in Fig. 7).

Second, there is a structurally resolvable integration of the nucleus fibres with the cartilaginous endplate (region C

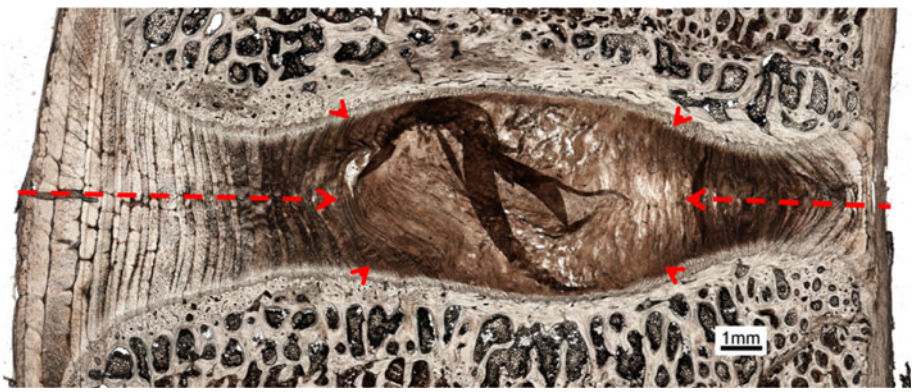

Fig. 3 Low magnification view of a sagittal section taken from an intact motion segment. Approximate boundary of the nucleus is indicated with *arrow heads*. The *red lines* indicate the approximate extent of ring severing

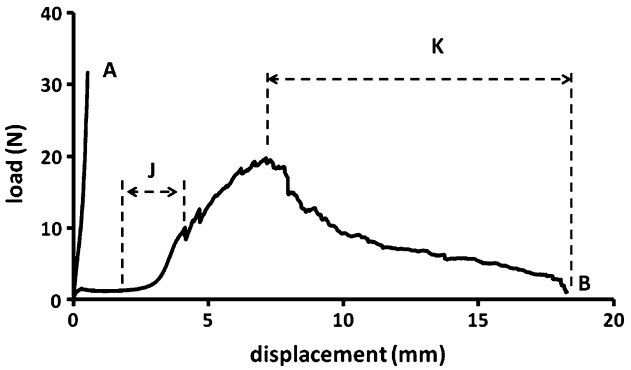

Fig. 4 Difference in response between the unsevered (*curve A*) and severed (*curve B*) samples. Note that loading of the unsevered samples was restricted to about 30 N due to limitations associated with gripping the sample in the testing machine

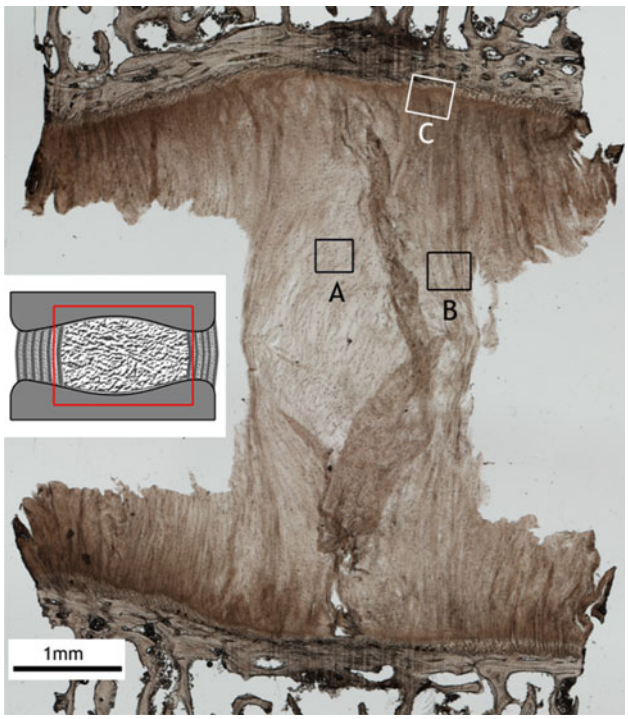

Fig. 5 Low magnification view of a ring-severed sample, showing the elongation of the nucleus region. The *inset* schematic indicates approximate region of interest in the intact disc. Higher magnification views of the *boxed regions A*, *B*, and *C* are shown in Figs. 6, 7, and 8. The extraneous flaps of tissue arise from the difficulty of sectioning the nucleus region

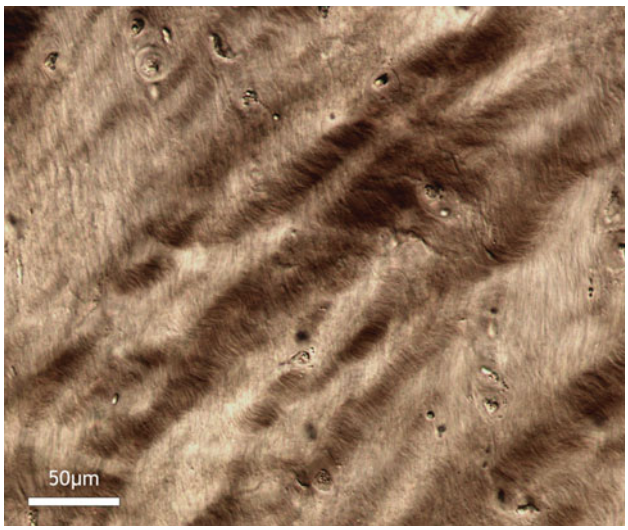

Fig. 6 High magnification view of fibres in *boxed region A* of Fig. 5, i.e. near the central nucleus. The strongly convoluted/crimped appearance of the fibres indicates that they are still moderately relaxed despite the 350% extension of the nucleus

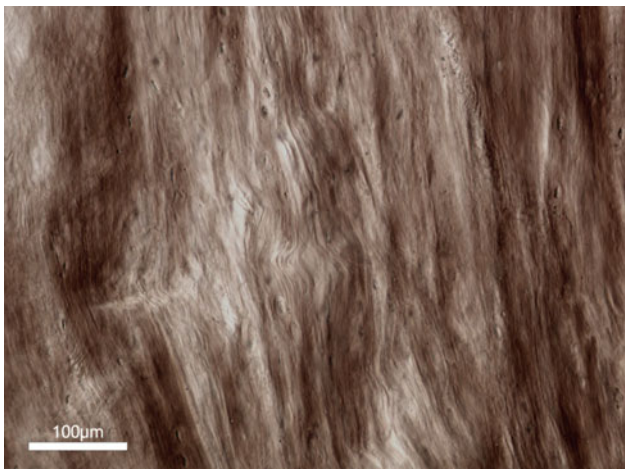

Fig. 7 Axially aligned (i.e. stretched) fibres near the nucleus edge region but further in from the endplate as in *boxed region B* in Fig. 5

in Fig. 5). This integration is visible both as discrete fibrous insertion nodes and as a more distributed form. The nodal form of insertion is shown in Fig. 8 (enlarged in Fig. 9). Viewed within a given section these nodes varied in density along the endplate/nucleus junction, tending to be less frequent (though still present) in the most central region and penetrating the cartilaginous endplate to varying depths. Further, these nodes were also present in the unstretched samples, as shown in Fig. 10, the difference being that the fibres immediately above the insertion boundary in the unstretched nucleus did not display the characteristic tautness of those fibres in the nodes in the stretched samples (compare Figs. 9, 10). The absence of such insertion nodes in any one region of the nucleus-endplate did not, however, imply an absence of nucleus-endplate integration. Figure 11 is an example of one such node-free region and clearly shows the more distributed nucleus fibrosity streaming into the cartilaginous endplate.

To reinforce the point that we have accurately represented the nucleus-endplate morphology in the above images, Fig. 12 shows a typical sagittal view of the mid annulus-endplate junction taken from an intact disc. The

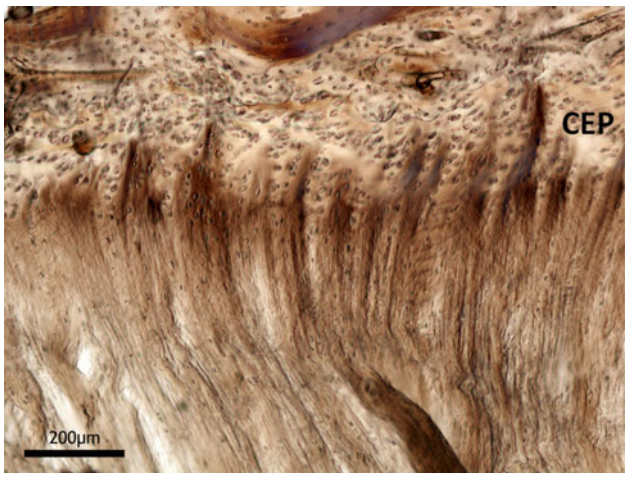

Fig. 8 Discrete insertion nodes in boxed *region C* in Fig. 5, showing the deep attachment of the nucleus fibres into the cartilaginous endplate (*CEP*)

distinctly alternating appearance of the oblique and counter-oblique layers up to their insertion in the endplate provides a striking morphological contrast with the modes of insertion observed in the nucleus-endplate region proper (e.g. Fig. 8). In the latter, such alternation is completely absent whether viewed in their stretched or unstretched state. This very different morphology provides further evidence that the substantial extension that occurs following ring-severing arises from the unravelling of the highly convoluted fibrosity characterising the unstretched nucleus.

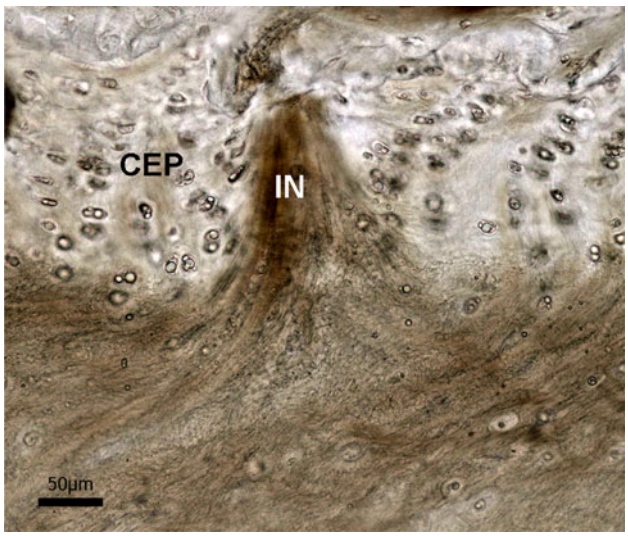

Fig. 10 Insertion node (*IN*) entering cartilaginous endplate (*CEP*) but imaged in an unstretched sample. Due to the fully relaxed state of the nucleus fibres, they lack the obvious axial alignment clearly visible in the stretched nucleus (c.f. Figs. 8, 9)

Discussion

As mentioned in our introduction the current literature presents a number of contrasting views on the extent and manner of integration of the nucleus with the endplate [20–25]. We believe this absence of a structural consensus has arisen because of the lack of a suitable experimental method to remove the influence of the annulus on nucleus

Fig. 9 High magnification view of the discrete insertion nodes shown in Fig. 8

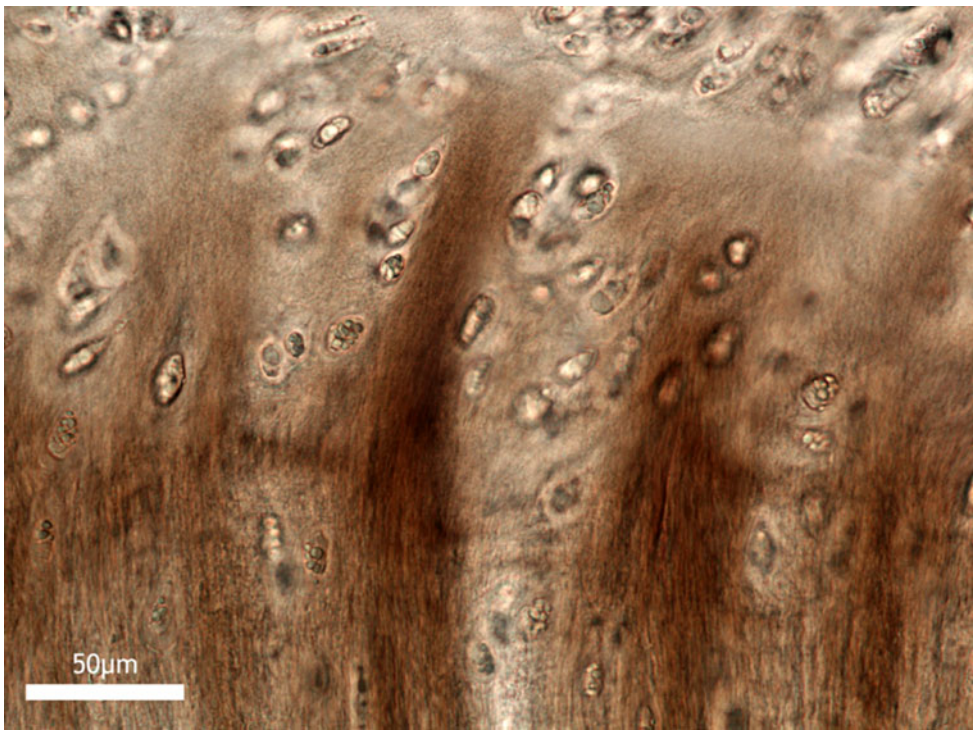

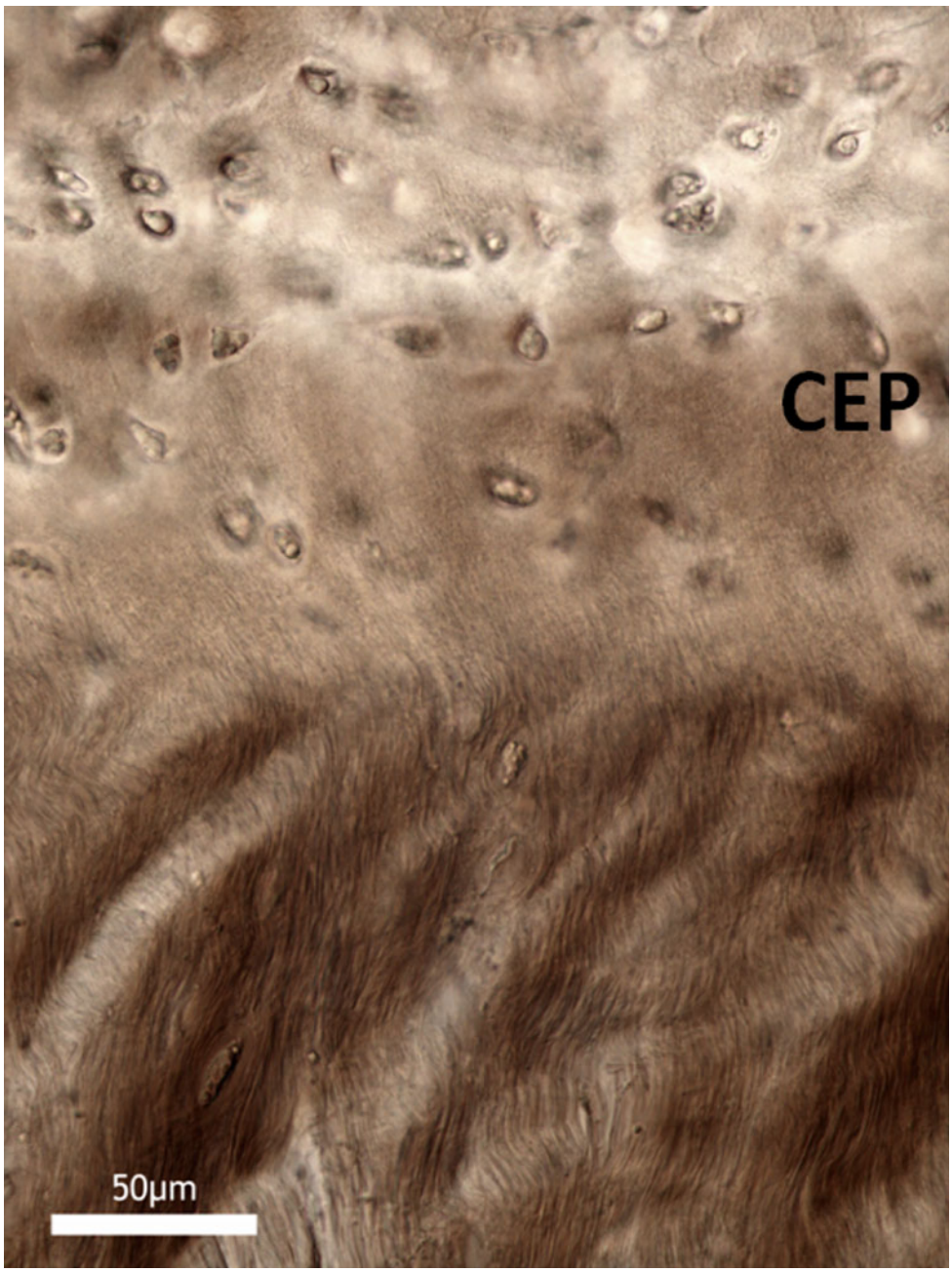

Fig. 11 Distributed nucleus fibrosity streaming into the cartilaginous endplate in a node-free region

unravelling. The novel ring-severing technique employed in this new study has enabled us to examine more critically the nature of nucleus-endplate integration.

It should be noted that although the transition between outer nucleus and inner annulus is structurally somewhat vague, our study employed two distinct discriminating criteria that enabled us to define the remaining material as essentially nucleus. First, the sudden large extension observed following ring-severing confirmed the functional dislocation of all fibres that had contributed to the strain-restricting properties of the unsevered annulus arising from its cross-ply lamellar structure. Secondly, the obvious morphological difference in endplate insertion morphology between the nucleus and annular regions (c.f. Figs. 8, 11 with Fig. 12) confirmed that the samples in their ring-severed state represented the behaviour of the isolated nucleus.

The ring-severing procedure we have used in this study allows the nucleus as defined above to be loaded directly in tension. The dramatic extension that precedes the point of rapid increase in modulus (see region J on curve B in Fig. 5) is clear confirmation that the nucleus possesses some form of structural continuity, is highly convoluted, is fully integrated with the endplates via two modes of direct

Fig. 12 High magnification sagittal view of the mid annular-endplate junction. The obliquely cut alternating fibres comprising adjacent lamellae provide a contrasting morphology to that observed in the nucleus-endplate region (c.f. Figs. 8, 9)

fibrous insertion (see Figs. 8, 11), and has an intrinsic tensile strength. Following the phase of easy extension and rapid stiffening (the "J" region in Fig. 4), there is a progressive but irregular rise to the peak load with eventual failure preceded by a gradual though erratic drop in load, and further large extension of the nucleus mass (region K in Fig. 4). This irregular form of the load–displacement curve suggests that the fibres within the nucleus region have varying degrees of convolution (and thus have varying extendable lengths) and hence are being loaded and ruptured sequentially rather than simultaneously.

Our images clearly indicate that nearer the nucleus edge of the stretched ring-severed tissue the fibres have become strongly aligned in the stretching direction (see region in box B in Fig. 5 and enlarged in Fig. 7), thus confirming that there is endplate-to-endplate load transmission by these fibres. This ability to transmit force obviously implies some form of structural continuity of the fibres themselves. In fact this continuity nearer the nucleus edge was readily observed and recorded using multiple image maps (each >50 images), but for practical reasons could not be included in our data presentation. Also, due to the inability of light microscopy to image individual collagen fibrils the present study cannot confirm the exact basis of this structural continuity. Whether fibrils themselves run continuously from endplate to endplate, or whether the fibres are constructed from shorter lengths of overlapping fibrils remains an unresolved question.

Although we were unable to image microscopically the final stages of nucleus rupture because of the extreme fragility of the remaining highly necked tissue, we assume that the diminishing mechanical strength in the post peak load region (region K in Fig. 4) is a direct consequence of the slightly less convoluted outer nucleus fibres being overloaded, then failing and thus transferring the applied load into the next inner cohort of fibres, these in turn possessing a slightly higher level of convolution, etc. This mechanism of sequential rupture of the nucleus fibres is illustrated schematically in Fig. 13a–d.

That the nucleus has resistance to tension when it clearly operates in compression raises the question as to why it might possess this tensile property. It should be emphasized that we have used tensile stretching to demonstrate the existence of endplate-to-endplate structural/mechanical cohesion. However, during normal disc function in vivo the nucleus fibres will not see this tensile mode of loading. We therefore suggest that the integration of the fibres with the endplates acts to provide the nucleus with a form of *tethered mobility*. In this way the fibres would function (1) to contain the proteoglycans via some form of collagen–proteoglycan interaction so as to maintain the hydration potential of the nucleus [26, 27], and (2) to provide a substrate for the cells within the nucleus so as to maintain an appropriate biology. The convoluted geometry of the fibres would still confer a high degree of freedom so as to accommodate nucleus shape changes associated with normal disc function in which hydrostatic loading plays an essential role [5].

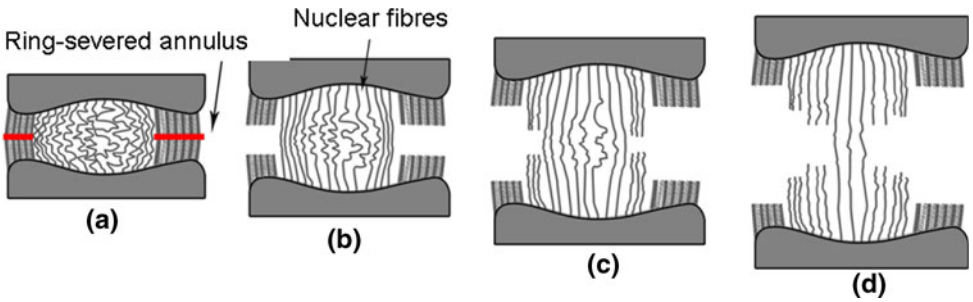

Fig. 13 **a–d** Illustrates schematically the effect of ring-severing and stretching on the morphological response of the nucleus fibres. Note how the longest, most convoluted fibres in the middle of the nucleus progressively unfold with increasing extension while the shorter fibres on the edge of the nucleus are the first to undergo tensile realignment and then failure

In summary, the present study provides new insights into what constitutes a normal nucleus-endplate structural relationship, at least in the mature ovine spine. It offers a structural framework for exploring how early degenerative changes might alter the nucleus-endplate relationship. Our results provide a contrasting view to much of the published literature which either states that there is no significant connection between the nucleus and endplate, or largely ignores the issue. Our experiments, demonstrating that the central nucleus alone is capable of carrying substantial tensile loads, provide clear evidence that it is highly structured, though convoluted, and hence can give the appearance of disorder to the casual observer using standard sectioning planes.

Conclusions

The ovine nucleus possesses a distinct fibrosity which displays structural continuity from endplate to endplate. This fibrosity is structurally integrated with the cartilaginous endplates and is capable of withstanding significant tensile forces. A structured though convoluted, tethered nucleus model is proposed that supports the general concept of a relatively mobile nucleus behaving hydrostatically within the confinement of the annulus.

Acknowledgments The authors are grateful for the award of funding in support of this research from both the Wishbone Trust (New Zealand Orthopaedic Association) and the University of Auckland.

References

1. Humzah MD, Soames RW (1988) Human intervertebral disc: structure and function. Anat Rec 220:337–356
2. Adams MA (2004) Biomechanics of back pain. Acupunct Med 22:178–188
3. Coventry MB, Ghormley, Ralph K, Kernohan, James W (1945) The intervertebral disc: its microscopic anatomy and pathology part I. Anatomy, Development and Physiology. The J Bone Joint Surg XXVII
4. Cassidy JJ, Hiltner A, Baer E (1989) Hierarchical structure of the intervertebral disc. Connect Tissue Res 23:75–88
5. Hukins DWL, Meakin JR (2000) Relationship between structure and mechanical function of the tissues of the intervertebral joint. Am Zool 40:42–52
6. Adams MA, McMillan DW, Green TP, Dolan P (1996) Sustained loading generates stress concentrations in lumbar intervertebral discs. Spine 21:434–438
7. Nachemson A (1975) Towards a better understanding of low back pain: a review of the mechanics of the lumbar disc. Rheumatol Rehabil 14:129–143
8. Urban JPG, Roberts S, Ralphs JR (2000) The nucleus of the intervertebral disc from development to degeneration. Am Zool 40:53–61
9. Adams MA, Green TP (1993) Tensile properties of the annulus fibrosus. I. The contribution of fibre-matrix interactions to tensile stiffness and strength. Eur Spine J 2:203–208
10. Green TP, Adams MA, Dolan P (1993) Tensile properties of the annulus fibrosus. II. Ultimate tensile strength and fatigue life. Eur Spine J 2:209–214
11. Galante JO (1967) Tensile properties of the human lumbar annulus fibrosus. Acta Orthop Scand
12. Holzapfel GA, Schulze-Bauer CAJ, Feigl G, Regitnig P (2005) Single lamellar mechanics of the human lumbar anulus fibrosus. Biomech Model Mechanobiol 3:125–140
13. Pezowicz CA, Robertson PA, Broom ND (2006) The structural basis of interlamellar cohesion in the intervertebral disc wall. J Anat 208:317–330
14. Pezowicz CA, Robertson PA, Broom ND (2005) Intralamellar relationships within the collagenous architecture of the annulus fibrosus imaged in its fully hydrated state. J Anat 207:299–312
15. Schollum ML, Robertson PA, Broom ND (2009) A microstructural investigation of intervertebral disc lamellar connectivity: Detailed analysis of the translamellar bridges. J Anat 214:805–816
16. Schollum ML, Robertson PA, Broom ND (2008) ISSLS prize winner: microstructure and mechanical disruption of the lumbar disc annulus: part I: a microscopic investigation of the translamellar bridging network. Spine 33:2702–2710
17. Yu J, Peter C, Roberts S, Urban JPG (2002) Elastic fibre organization in the intervertebral discs of the bovine tail. J Anat 201:465–475
18. Yu J, Tirlapur U, Fairbank J, Handford P, Roberts S, Winlove CP, Cui Z, Urban J (2007) Microfibrils, elastin fibres and collagen fibres in the human intervertebral disc and bovine tail disc. J Anat 210:460–471
19. Buckwalter JA, Cooper RR, Maynard JA (1976) Elastic fibers in human intervertebral discs. J Bone Joint Surg Ser A 58:73–76
20. Inoue H (1981) Three-dimensional architecture of lumbar intervertebral discs. Spine 6:139–146
21. Inoue H, Takeda T (1975) Three dimensional observation of collagen framework of lumbar intervertebral discs. Acta Orthopaed Scand 46:949–956
22. Takeda T (1975) Three dimensional observation of collagen framework of human lumbar discs. J Jap Orthop Ass 49:45–57
23. Roberts S, Menage J, Urban JPG (1989) Biochemical and structural properties of the cartilage end-plate and its relation to the intervertebral disc. Spine 14:166–174
24. Melrose J, Smith SM, Little CB, Moore RJ, Vernon-Roberts B, Fraser RD (2008) Recent advances in annular pathobiology provide insights into rim-lesion mediated intervertebral disc degeneration and potential new approaches to annular repair strategies. Eur Spine J 17:1131–1148
25. Vernon-Roberts B, Moore RJ, Fraser RD (2007) The natural history of age-related disc degeneration: the pathology and sequelae of tears. Spine 32:2797–2804
26. Raj PP (2008) Intervertebral disc: anatomy–physiology–pathophysiology-treatment. Pain Pract 8:18–44
27. Heinegard D (2009) Proteoglycans and more—from molecules to biology. Int J Exp Pathol 90:575–586